

Crystal chemistry of Cr³⁺-V³⁺-rich clinopyroxenes

L. SECCO,^{1,*} F. MARTIGNAGO,¹ A. DAL NEGRO,¹ L.Z. REZNITSKII,² AND E.V. SKLYAROV ²

¹Dipartimento di Mineralogia e Petrologia, Università di Padova, Corso Garibaldi 37, Padova, Italy

²Russian Academy of Science. Siberian Branch, Institute of the Earth's Crust, Lermontova Street, 128, Irkutsk, Russia

ABSTRACT

Eleven clinopyroxenes from the Sludyanka Crystalline Complex in Russia belonging to the ternary join NaVSi₂O₆-NaCrSi₂O₆-CaMgSi₂O₆ (natalyite-kosmochlor-diopside) were studied by means of X-ray single crystal diffractometry and electron probe microanalysis.

The crystal chemical data show that the T site is almost completely occupied by Si, so that the Na (V³⁺,Cr³⁺) → Ca Mg substitution mechanism ensures charge balance. Changes in M1 site geometry are explained by the aggregate ionic radius, and are influenced by Mg occupancy and V³⁺/(V³⁺ + Cr³⁺) ratio. The M2 site geometry depends both on Na content and on the (V³⁺,Cr³⁺) → Mg substitution in M1 site. Changes in M2-O3c1 bond length are mainly related to Na content, whereas the longest M2-O3c2 bond lengths are significantly affected by the V³⁺/(V³⁺ + Cr³⁺) ratio of the M1 site. The T site geometry is affected by chemical and geometrical variations at the M1 and M2 sites, principally the M1 site occupancy.

INTRODUCTION

Chromium-bearing clinopyroxenes are relatively widespread in meteorites and terrestrial rocks. Most of them belong to the kosmochlor-aegirine-jadeite-augite system and some to the kosmochlor-diopside binary join. Great interest in kosmochlor-bearing pyroxene solid solutions has been aroused by the possibility of using Cr³⁺ contents in natural pyroxenes to estimate the *P-T* conditions of formation of meteorites, lunar, and mantle rocks. Natalyite (NaVSi₂O₆), was found in the Sludyanka Crystalline Complex, Russia (Reznitskii et al. 1985), and the complete NaVSi₂O₆-NaCrSi₂O₆-CaMgSi₂O₆ ternary solid solution was later described in the same rocks (Reznitskii et al. 1998, 1999). The present study was undertaken to give further data and crystal chemical details on natural V and Cr-rich clinopyroxenes, because no data exist in the literature, except for the synthetic end-members natalyite (Ohashi et al. 1994), kosmochlor (Clark et al. 1969), and the solid solution diopside-kosmochlor (Ohashi and Fujita 1979). The aim of this work is to describe the crystal chemistry of a natural series of clinopyroxene characterized by variable extents of the Na → Ca and (V³⁺,Cr³⁺) → Mg substitutions, and to analyze the M1, M2, and T site geometry variations as a function of the mean ionic radius (I.R.) of the octahedral cations.

GEOLOGICAL SETTING AND OCCURRENCE OF Cr-V-BEARING PYROXENES

The metamorphic rocks of the southwestern shore of Lake Baikal are known as the Sludyanka Complex which, being situated near the boundary of the Siberian craton, is considered to be part of the Central Asian foldbelt. Sludyanka metamorphism corresponds to granulite facies of moderate pressure (maximum *P-T* conditions: *T* = 800–830 °C, *P* = 6–8 kbar).

The Cr-V mineral assemblage is related to a certain

lithological type of metasediment, generally considered as quartz-diopside. The latter has a simple chemical and mineralogical composition, and consists of pure white diopside, quartz, calcite, and sometimes rock-forming apatite.

Thin layers and lenses of Cr-V-bearing varieties [(Cr₂O₃ + V₂O₃) 0.1–0.7 wt%, rarely up to 1–2 wt%] sometimes occur irregularly within bands of the quartz-diopside rock type. The Cr/V ratio in these layers and lenses varies from 15:1 to 1:6. These rocks contain a wide range of Cr-V silicates and opaque minerals, always including Cr-V-bearing pyroxenes (Reznitskii and Sklyarov 1996).

Three morphological types of clinopyroxene are distinguished: (1) rock-forming Cr-V-bearing diopside; (2) Cr-V-bearing pyroxene forming rims around esclaite-karelianite inclusions in diopside (Reznitskii et al. 1998); (3) Cr-V-pyroxenes, occurring as inclusions in lenses and veins of quartz (Reznitskii et al. 1985). The pyroxenes of this work belong to the third type.

There are good correlations between Na and (Cr³⁺ + V³⁺), corresponding to Na (Cr³⁺,V³⁺) → Ca Mg exchange. Diopside, kosmochlor and natalyite are the main components (90–99 mol%) of the pyroxenes and a nearly complete solid solution CaMgSi₂O₆-NaCrSi₂O₆-NaVSi₂O₆ was found (Fig. 1).

EXPERIMENTAL METHODS

X-ray single crystal diffraction

Eleven clinopyroxene crystals, optically homogeneous, inclusion-free, and with sharp diffraction profiles, were hand-picked for single-crystal X-ray diffraction.

Intensity data were collected up to 2θ = 70° (MoKα radiation monochromatized by a flat graphite crystal) using a SIEMENS AEDII four-circle automated diffractometer. The intensities of the *hkl* and $\bar{h}\bar{k}l$ reflections and of their monoclinic equivalents $h\bar{k}l$ and $\bar{h}kl$, were measured using ω-2θ scan mode and were corrected for absorption following the Ψ scan method of North et al. (1968).

* E-mail: luciano@dmp.unipd.it

Unit-cell parameters were measured after each data collection by centering 30 selected reflections at both positive and negative 2 θ angles using the double-step scan routine.

Structure refinements based on F_o^2 were performed using the SHELXL-97 program, an updated version of SHELXL-93 (Sheldrick 1993), in space group $C2/c$ without chemical constraints. The values of the equivalent pairs were averaged and the resulting discrepancy factors R_{int} are reported in Table 1.

The atomic scattering curves were taken from the International Tables for X-Ray Crystallography (Ibers and Hamilton 1974) and from Tokonami (1965). Complete ionization of the cations at the M1 (Mg²⁺, Cr³⁺, and/or V³⁺) and M2 (Ca²⁺, Na⁺) sites was adopted.

The ionization states of the Si and O atoms were considered as variables using a linear combination of xf (Si) + $(1-x)f$ (Si⁴⁺) and xf (O) + $(1-x)f$ (O²⁻), x being a variable. The results led to approximate ionization states of 1.2⁻ for bridging O atoms, 1.5⁻ for non-bridging O atoms, and 1.8⁺ for silicon atoms.

Extinction correction was done according to Sheldrick (1993).

The weighting scheme used is defined as $w = 1/[(\sigma^2(F_o^2) + (AP)^2 + BP)]$ where $P = (F_o^2 + 2F_c^2)/3$. A and B were chosen for

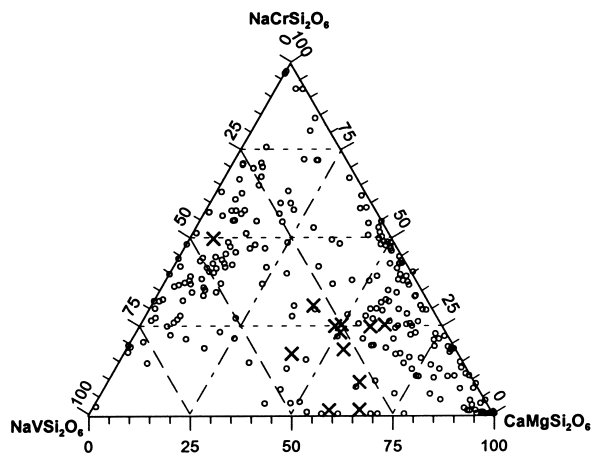


FIGURE 1. Natalyite-kosmochlor-diopside ternary diagram showing compositions of Sludyanka pyroxenes. Crosses = compositions of pyroxenes listed in Table 5.

TABLE 1. Refinement data from X-ray single-crystal diffraction

Sample	1	2	3	4	5	6
a (Å)	9.6072 (5)	9.6595(14)	9.6631 (5)	9.6582 (15)	9.6718 (7)	9.6774 (6)
B (Å)	8.7413 (6)	8.8263(17)	8.8263 (6)	8.8273 (18)	8.8412 (9)	8.8479 (8)
c (Å)	5.2771 (2)	5.2686 (6)	5.2709 (2)	5.2665 (6)	5.2670 (3)	5.2662 (3)
β (°)	107.172 (4)	106.596 (12)	106.601 (4)	106.577 (13)	106.483 (6)	106.446 (6)
V (Å ³)	423.41	430.48	430.81	430.34	431.87	432.47
Total refl.	2013	2029	2082	2073	2082	2088
Unique refl.	933	957	959	955	959	962
R_{int} (%)	1.4	2.2	2.4	1.4	1.6	1.3
R (%)	1.7	1.8	2.3	1.6	1.7	1.6
WR (%)	3.5	4.4	3.7	3.4	4.1	3.7
m.a.n. M1cryst	22.49 (11)	18.65 (10)	18.68 (12)	18.10 (9)	17.91 (10)	17.30 (9)
m.a.n. M1chem	22.52	18.90	18.49	17.73	17.70	17.18
m.a.n. M2cryst	11.43 (12)	14.48 (13)	14.38 (14)	14.71 (11)	15.15 (13)	15.54 (11)
m.a.n. M2chem	11.50	14.72	14.76	15.17	15.58	15.85

Note: Standard deviations are in parentheses. m.a.n. = mean atomic number.

$$R_{int} = \sum |F_o^2 - \overline{F_o^2}| / \overline{F_o^2} \quad R = \sum |F_o - |F_c|| / \sum |F_o| \text{ for } F_o^2 > 2\sigma(F_o^2) \quad wR = \sqrt{\sum w(F_o^2 - F_c^2)^2 / \sum w(F_o^2)^2}$$

each crystal to produce a flat analyses of variance in terms of F_o^2 , as suggested by SHELXL-97.

All parameters were refined simultaneously, and no correlation greater than 0.6 between site occupancies and thermal parameters was observed.

The Fourier difference map did not show residual electron density peaks, precluding the existence of the split site M2' (Dal Negro et al. 1982) which would indicate the presence of cations with ionic radii significantly smaller than those of Na and Ca.

Unit-cell parameters, the number of total and unique reflections, the conventional discrepancy indices R [based on $F_o^2 > 2\sigma(F_o^2)$] and wR (based on all the F_o^2) are listed in Table 1.

The geometrical parameters are given in Table 2, and the final positional and displacement parameters are reported in Table 3. Observed and calculated structure factors have been deposited (Table 4¹).

Microprobe analysis

Chemical analyses were performed on thin polished sections of the crystals used for X-ray data collection, using a CAMECA-CAMEBAX electron microprobe operating with a fine-focused beam (~1 μ m) at 15 kV and 20 nA sample current in wavelength-dispersive mode (WDS), with 20 s counting times for both peak and total background. Synthetic pure oxides were used as standards for Mg, Al, Ti, Cr, Mn, and Fe, wollastonite for Si and Ca, albite for Na, and vanadinite for V. Using the PAP correction program supplied by CAMECA, X-ray counts were converted into oxide weight percentages. No systematic compositional variations were observed in the crystals.

Bulk compositions, obtained by averaging 20 microprobe spots for each single crystal, and site partitioning are listed in Table 5. The cation content obtained, based on four cations and six O atoms, were distributed by combining the results of structure refinement and electron probe analysis according to Dal Negro et al. (1982).

¹For a copy of Table 4, document item AM-02-008, contact the Business Office of the Mineralogical Society of America for price information. Deposit items may also be available on the American Mineralogist web site (<http://www.minsocam.org>).

TABLE 2. Bond distances (Å), volume (Å³) of polyhedra, and other geometrical parameters

Sample	1	2	3	4	5	6
M1-O2	1.9504 (7)	1.9886 (7)	1.9873 (8)	1.9878 (6)	1.9958 (7)	1.9991 (6)
M1-O1A2	2.0296 (7)	2.0389 (7)	2.0417 (8)	2.0377 (6)	2.0418 (7)	2.0426 (6)
M1-O1A1	2.0543 (7)	2.0846 (7)	2.0876 (8)	2.0850 (6)	2.0918 (7)	2.0928 (6)
<M1-O>	2.0114 (17)	2.0373 (17)	2.0389 (20)	2.0368 (15)	2.0431 (17)	2.0448 (15)
V _{M1}	10.722 (2)	11.157 (2)	11.182 (3)	11.148 (2)	11.255 (2)	11.285 (2)
M2-O2	2.3859 (7)	2.3737 (7)	2.3760 (9)	2.3755 (6)	2.3732 (7)	2.3714 (6)
M2-O1	2.3785 (7)	2.3866 (7)	2.3875 (9)	2.3872 (6)	2.3861 (7)	2.3866 (6)
M2-O3c1	2.4294 (7)	2.4869 (7)	2.4846 (9)	2.4880 (6)	2.4961 (7)	2.5002 (6)
M2-O3c2	2.7852 (7)	2.7465 (7)	2.7563 (9)	2.7483 (6)	2.7437 (7)	2.7432 (6)
<M2-O>	2.4947 (20)	2.4984 (20)	2.5011 (25)	2.4997 (17)	2.4998 (20)	2.5004 (17)
V _{M2}	25.565 (4)	25.739 (4)	25.818 (5)	25.777 (3)	25.790 (4)	25.802 (3)
Δ _{M2}	0.387	0.331	0.340	0.331	0.325	0.324
T-O2	1.5919 (7)	1.5910 (7)	1.5894 (9)	1.5912 (6)	1.5897 (7)	1.5900 (6)
T-O1	1.6311 (7)	1.6206 (7)	1.6192 (9)	1.6183 (6)	1.6178 (7)	1.6166 (6)
T-O3A1	1.6385 (7)	1.6507 (7)	1.6500 (9)	1.6498 (6)	1.6533 (7)	1.6544 (6)
T-O3A2	1.6488 (7)	1.6643 (7)	1.6619 (9)	1.6649 (6)	1.6669 (7)	1.6684 (6)
<T-O>	1.6276 (14)	1.6316 (14)	1.6301 (18)	1.6311 (12)	1.6319 (14)	1.6324 (12)
T-O _{no brg}	1.6115 (10)	1.6058 (10)	1.6043 (13)	1.6048 (8)	1.6037 (10)	1.6033 (8)
T-O _{brg}	1.6436 (10)	1.6575 (10)	1.6559 (13)	1.6574 (8)	1.6601 (10)	1.6614 (8)
V _T	2.200 (1)	2.214 (1)	2.209 (1)	2.212 (1)	2.215 (1)	2.216 (1)
O3-O3-O3 (°)	172.3	169.4	169.8	169.5	169.1	168.9

Note: Standard deviations are in parentheses.

ΔM2 = M2 - O3c2 - [(M2 - O3c1 + M2 - O1 + M2 - O2)/3].

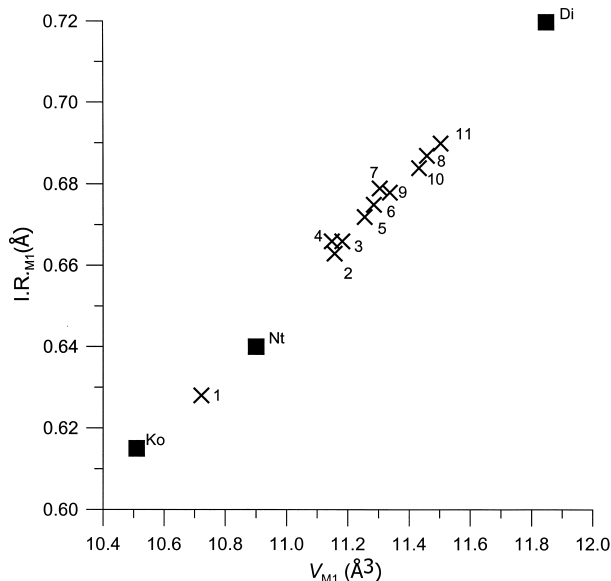


FIGURE 2. M1 site volume (V_{M1}) vs. $I.R._{M1}$. Crosses = this study; filled squares = synthetic clinopyroxenes from Clark et al. (1969) for Ko and Di and from Ohashi et al. (1994) for Nt.

RESULTS AND DISCUSSION

The clinopyroxenes studied belong to a natural series defined by the three end-members diopside (Di), natlyite (Nt), and kosmochlor (Ko) (Fig. 1). They are characterized by an M1 site occupied by Mg²⁺ (0.05–0.65 atoms per formula unit, apfu), Cr³⁺ (0.01–0.48 apfu) and V³⁺ (0.14–0.30 apfu) in variable proportions. Charge balance is almost completely attained by Na → Ca substitution in the M2 site, the T site being almost filled by Si (maximum ¹⁴¹Al content = 0.030 apfu).

Figure 2 shows a good correlation between the volume of the M1 site (V_{M1}) and the averaged ionic radius calculated based

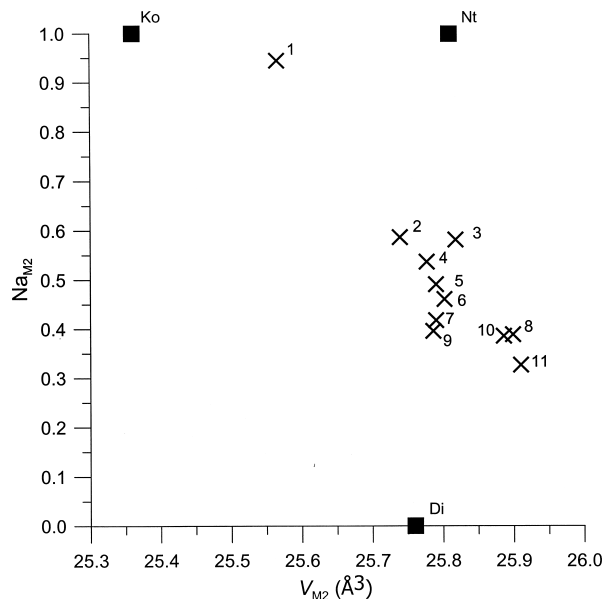


FIGURE 3. M2 site volume (V_{M2}) vs. Na_{M2} content. Symbols as in Figure 2.

on site occupancies. Given the values of the I.R. (Mg²⁺ = 0.72, Cr³⁺ = 0.615, V³⁺ = 0.64), the studied clinopyroxenes plot between the end-members Ko-Nt-Di and are characterized by geometrical variations of the M1 polyhedron due mainly to the Mg content. The effect of the V³⁺/(V³⁺+Cr³⁺) ratio is shown by samples 2–3 and 8–9, which have the same Mg content at M1.

As outlined above, the (V³⁺,Cr³⁺) → Mg²⁺ substitution at the M1 site is balanced by the Na → Ca substitution at the M2 site; therefore, the M2 site geometry is related not only to the Ca/(Ca + Na) ratio but also to the M1 site occupancy. In fact, as shown in Figure 3, the end-members Ko and Nt, with the

TABLE 3. Fractional coordinates and equivalent isotropic displacement parameters (\AA^2) for the structural sites

Sample		1	2	3	4	5
T	x	0.29165 (3)	0.28932 (3)	0.28940 (3)	0.28912 (2)	0.28887 (3)
	y	0.09132 (3)	0.09197 (3)	0.09181 (4)	0.09199 (2)	0.09210 (3)
	z	0.23581 (5)	0.23203 (5)	0.23283 (6)	0.23179 (4)	0.23163 (5)
	U_{eq}	0.00406 (7)	0.00455 (7)	0.00410 (9)	0.00432 (6)	0.00464 (7)
O1	x	0.11430 (8)	0.11451 (7)	0.11481 (9)	0.11457 (6)	0.11467 (7)
	y	0.07965 (8)	0.08201 (8)	0.08181 (11)	0.08184 (7)	0.08255 (8)
	z	0.13983 (14)	0.13990 (14)	0.14013 (17)	0.13966 (12)	0.14007 (14)
	U_{eq}	0.00598 (13)	0.00718 (13)	0.00675 (16)	0.00703 (11)	0.00736 (13)
O2	x	0.36076 (8)	0.36058 (8)	0.36049 (10)	0.36041 (6)	0.36041 (8)
	y	0.25718 (8)	0.25413 (8)	0.25395 (10)	0.25417 (7)	0.25353 (8)
	z	0.30565 (14)	0.31074 (14)	0.31026 (18)	0.31028 (12)	0.31131 (14)
	U_{eq}	0.00766 (14)	0.00857 (13)	0.00806 (18)	0.00837 (11)	0.00880 (14)
O3	x	0.35267 (8)	0.35176 (7)	0.35154 (10)	0.35165 (6)	0.35161 (7)
	y	0.01016 (8)	0.01384 (8)	0.01331 (10)	0.01373 (7)	0.01422 (8)
	z	0.00964 (14)	0.00207 (13)	0.00309 (18)	0.00211 (11)	0.00118 (13)
	U_{eq}	0.00688 (13)	0.00738 (13)	0.00694 (16)	0.00723 (11)	0.00765 (13)
M1	x	0	0	0	0	0
	y	0.90618 (3)	0.90580 (3)	0.90538 (5)	0.90568 (3)	0.90565 (3)
	z	0.25	0.25	0.25	0.25	0.25
	U_{eq}	0.00453 (8)	0.00514 (10)	0.00506 (12)	0.00498 (8)	0.00538 (10)
M2	x	0	0	0	0	0
	y	0.30078 (7)	0.30198 (5)	0.30170 (6)	0.30179 (4)	0.30199 (4)
	z	0.25	0.25	0.25	0.25	0.25
	U_{eq}	0.01105 (25)	0.00914 (17)	0.00973 (20)	0.00941 (14)	0.00932 (16)

Note: Standard deviations are in parentheses.

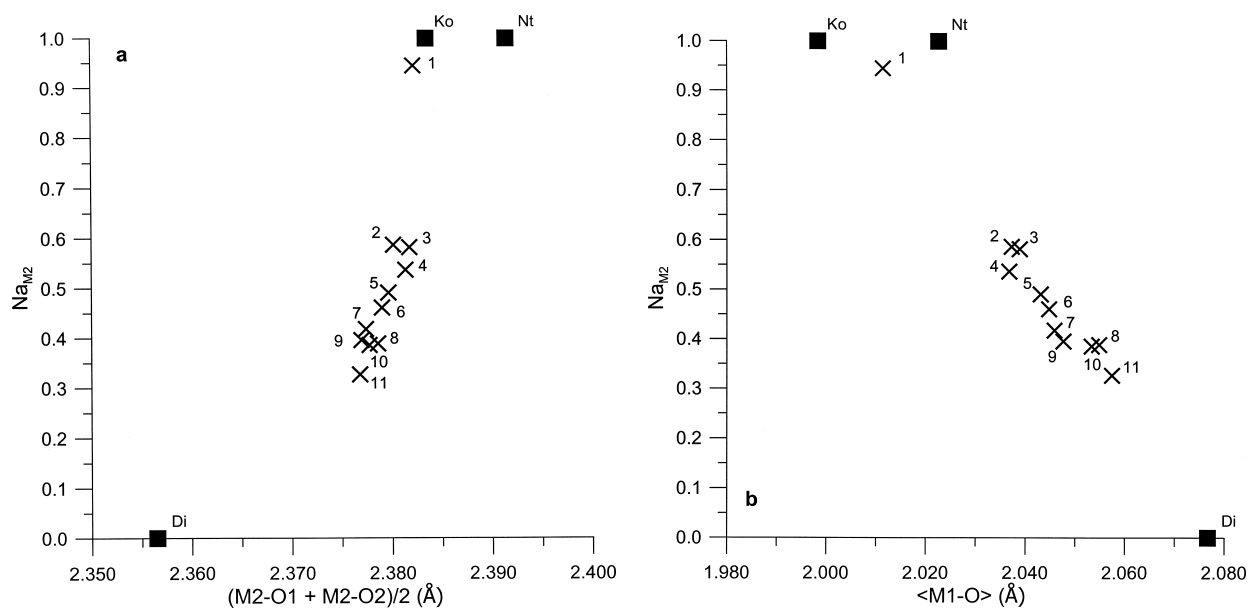


FIGURE 4. (a) $(M2-O1 + M2-O2)/2$ bond lengths vs. Na_{M2} content and (b) $\langle M1-O \rangle$ bond lengths vs. Na_{M2} content. Symbols as in Figure 2.

same Na content but with different cations at the M1 site, differ significantly in their V_{M2} . Excluding sample 1, which is intermediate between Ko and Nt, the other clinopyroxenes, with Na content decreasing from samples 2 to 11, are scattered over a field outside the expected one. Considering the pairs 2–3 and 8–9 (each with the same Na and Mg contents at the M2 and M1 sites), the V_{M2} increase is due to an increase in the $V^{3+}/(V^{3+}+Cr^{3+})$ ratio at the M1 site. In the two end-members Nt and Di (the

former with Na at M2 and V at M1, the latter with Ca at M2 and Mg at M1), V_{M2} is surprisingly similar. This is due to the shortening of the M2-O1, M2-O2, and M2-O3c2 bond lengths and to the lengthening of M2-O3c1 bond lengths for Di compared to Nt. Di shows the shortest M2-O1 and M2-O2 bond lengths (Fig. 4a) and the longest $\langle M1-O \rangle$ bond length (Fig. 4b). Sample 1, which plots between the Ko and Nt end-members in the other plots, has shorter bond lengths than Ko and

TABLE 3.— *extended*

6	7	8	9	10	11
0.28864 (2)	0.28839 (3)	0.28821 (3)	0.28819 (2)	0.28816 (3)	0.28785 (5)
0.09214 (2)	0.09234 (3)	0.09221 (3)	0.09236 (3)	0.09227 (3)	0.09235 (5)
0.23137 (4)	0.23071 (5)	0.23143 (5)	0.23042 (4)	0.23104 (6)	0.23090 (9)
0.00432 (7)	0.00416 (7)	0.00427 (7)	0.00425 (6)	0.00417 (8)	0.00430 (12)
0.11470 (7)	0.11459 (7)	0.11514 (7)	0.11480 (6)	0.11511 (8)	0.11516 (12)
0.08259 (7)	0.08294 (8)	0.08339 (8)	0.08323 (7)	0.08351 (9)	0.08387 (14)
0.14011 (12)	0.13969 (14)	0.14097 (14)	0.13995 (12)	0.14056 (15)	0.14066 (25)
0.00691 (11)	0.00698 (13)	0.00696 (13)	0.00709 (11)	0.00668 (14)	0.00677 (23)
0.36050 (7)	0.36041 (8)	0.36061 (8)	0.36041 (7)	0.36047 (9)	0.36054 (14)
0.25325 (7)	0.25296 (8)	0.25228 (8)	0.25281 (7)	0.25246 (9)	0.25190 (14)
0.31172 (12)	0.31201 (14)	0.31283 (14)	0.31211 (13)	0.31251 (16)	0.31329 (26)
0.00847 (12)	0.00811 (14)	0.00825 (13)	0.00838 (12)	0.00819 (15)	0.00825 (24)
0.35159 (6)	0.35141 (7)	0.35126 (7)	0.35137 (6)	0.35116 (8)	0.35106 (13)
0.01436 (7)	0.01474 (8)	0.01478 (8)	0.01499 (7)	0.01483 (9)	0.01524 (14)
0.00085 (11)	-0.00011 (14)	0.00004 (13)	-0.00056 (12)	-0.00009 (15)	-0.00050 (25)
0.00714 (11)	0.00688 (13)	0.00715 (13)	0.00684 (11)	0.00695 (14)	0.00691 (23)
0	0	0	0	0	0
0.90572 (3)	0.90599 (4)	0.90551 (4)	0.90619 (3)	0.90572 (4)	0.90577 (7)
0.25	0.25	0.25	0.25	0.25	0.25
0.00523 (9)	0.00446 (11)	0.00526 (11)	0.00451 (10)	0.00497 (12)	0.00536 (22)
0	0	0	0	0	0
0.30190 (4)	0.30190 (4)	0.30200 (4)	0.30199 (4)	0.30190 (5)	0.30200 (7)
0.25	0.25	0.25	0.25	0.25	0.25
0.00920 (14)	0.00916 (14)	0.00930 (14)	0.00906 (12)	0.00921 (15)	0.00961 (24)

TABLE 5. Microprobe analyses, unit formulae recalculation (six O atoms), and partitioning

Sample	1	2	3	4	5	6	7	8	9	10	11	12
SiO ₂	53.35	53.59	53.73	54.34	53.69	53.95	53.97	53.94	53.61	54.18	54.46	54.03
Al ₂ O ₃	0.75	0.30	0.92	1.06	0.80	0.67	0.88	0.62	0.65	0.23	0.70	0.49
MgO	1.00	7.02	7.30	8.41	8.80	8.87	9.56	10.13	10.63	10.68	11.08	11.87
FeO	0.03	0.35	0.10	0.00	0.23	0.36	0.00	0.40	0.10	0.26	0.10	0.16
TiO	0.11	0.00	0.04	0.00	0.00	0.04	0.00	0.00	0.11	0.04	0.00	0.07
MnO	0.03	0.03	0.00	0.00	0.03	0.03	0.00	0.00	0.00	0.06	0.00	0.03
Cr ₂ O ₃	16.13	10.17	5.65	8.19	8.46	7.65	6.12	8.28	0.34	8.44	3.04	0.38
V ₂ O ₃	14.24	9.59	13.60	8.72	8.24	8.69	9.33	6.03	13.60	4.75	9.54	10.93
CaO	1.37	10.40	10.55	11.75	12.90	12.88	13.68	14.75	15.50	15.35	15.65	17.15
Na ₂ O	13.00	8.17	8.12	7.53	6.85	6.87	6.47	5.85	5.45	5.56	5.44	4.60
Σ	100.01	99.61	100.01	100.00	100.00	100.01	100.01	100.00	99.99	99.55	100.01	99.71
T site												
Si	2.000	1.987	1.986	1.998	1.982	1.990	1.985	1.986	1.972	1.990	1.994	1.979
^{IV} Al	0.000	0.013	0.014	0.002	0.018	0.010	0.015	0.014	0.028	0.010	0.006	0.021
Σ	2.000	2.000	2.000	2.000	2.000	2.000	2.000	2.000	2.000	2.000	2.000	2.000
M1 site												
^{VI} Al	0.033	0.017	0.026	0.044	0.017	0.019	0.023	0.013	0.000	0.019	0.024	0.012
Mg	0.056	0.388	0.402	0.461	0.484	0.488	0.524	0.556	0.583	0.585	0.605	0.648
Fe ²⁺	0.001	0.011	0.003	0.000	0.007	0.011	0.000	0.012	0.003	0.008	0.003	0.005
Ti ⁴⁺	0.003	0.000	0.001	0.000	0.000	0.001	0.000	0.000	0.003	0.001	0.000	0.002
Mn ²⁺	0.001	0.001	0.000	0.000	0.001	0.001	0.000	0.000	0.000	0.002	0.000	0.001
Cr ³⁺	0.478	0.298	0.165	0.238	0.247	0.223	0.178	0.241	0.010	0.245	0.088	0.011
V ³⁺	0.428	0.285	0.403	0.257	0.244	0.257	0.275	0.178	0.401	0.140	0.280	0.321
Σ	1.000	1.000	1.000	1.000	1.000	1.000	1.000	1.000	1.000	1.000	1.000	1.000
I.R. (Å)	0.628	0.663	0.666	0.666	0.671	0.672	0.675	0.679	0.687	0.678	0.684	0.690
V ³⁺ /(V ³⁺ +Cr ³⁺)	0.472	0.489	0.710	0.519	0.497	0.535	0.607	0.425	0.976	0.364	0.761	0.967
M2 site												
Ca	0.055	0.413	0.418	0.463	0.510	0.509	0.539	0.582	0.611	0.604	0.614	0.673
Na	0.945	0.587	0.582	0.537	0.490	0.491	0.461	0.418	0.389	0.396	0.386	0.327
Σ	1.000	1.000	1.000	1.000	1.000	1.000	1.000	1.000	1.000	1.000	1.000	1.000

Note: I.R. = mean ionic radius from Shannon (1976).

Nt, because of lower amount of Mg and Ca at the M1 and M2 sites, respectively. Figure 5 shows a linear relationship between the M2-O3c1 distance and the Na_{M2} content. It should not be influenced by M1 site occupancy, because the Ko and Nt end-members have similar M2-O3c1 bond lengths. On the contrary

the M2-O3c2 bond length (Fig. 6) is affected by both M1 and M2 site occupancies. In this case, we observe that Ko and Nt differ in their M2-O3c2 bond lengths, and the natural clinopyroxenes, excluding sample 1, define two different trends as a function of V³⁺/(V³⁺+Cr³⁺) ratio; the first, for samples 11 to 2,

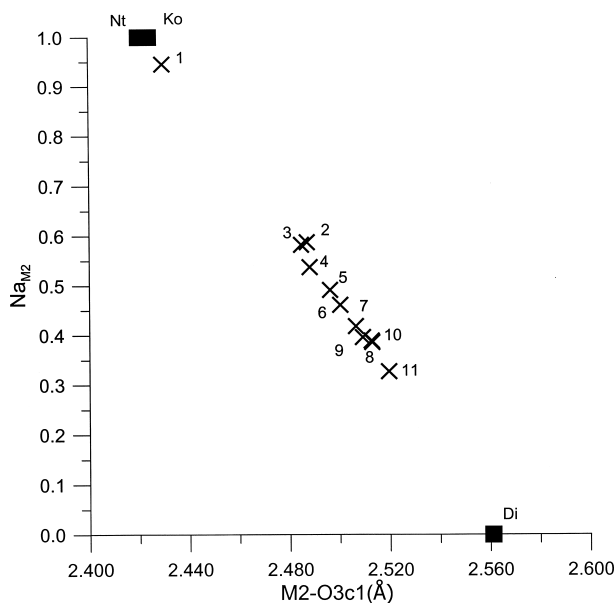


FIGURE 5. M2O-3c1 bond lengths vs. Na_{M2} content. Symbols as in Figure 2.

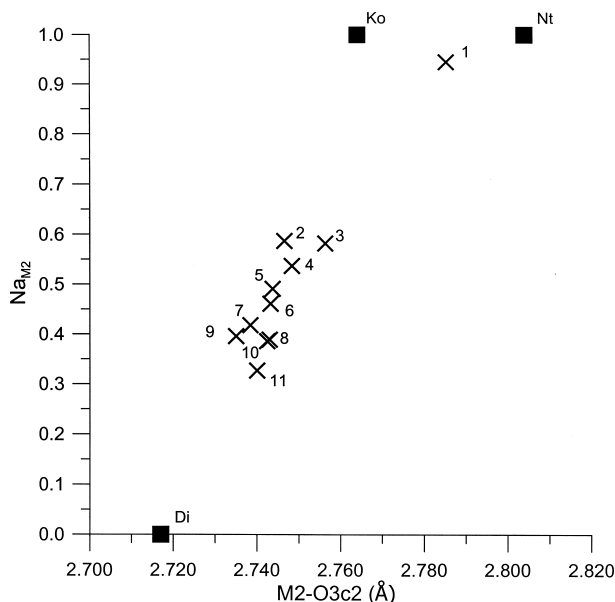


FIGURE 6. M2O-3c2 bond lengths vs. Na_{M2} content. Symbols as in Figure 2.

shows M2-O3c2 almost constant and low $V^{3+}/(V^{3+} + Cr^{3+})$ ratio. The second, from samples 10 to 3, shows significant M2-O3c2 lengthening because of a high $V^{3+}/(V^{3+} + Cr^{3+})$ ratio. In conclusion, the geometrical variations of the M2 polyhedron are influenced not only by its occupancy but also by that of the M1 site.

As observed by Ohashi (1981) changes in tetrahedral geometry are related to trivalent cations at the M1 site; the clinopyroxenes studied with T almost completely occupied by Si, are characterized by wide V_T and bond length variations which can be rationalized on the basis of M1 site occupancy (see Table 2).

ACKNOWLEDGMENTS

The authors especially thank R. Oberti for critical comments and helpful discussion that considerably improved this paper. This work benefited from the financial support of MURST (Transformations, reactions, ordering in minerals, 1999), CNR (Centro di Studio per la Geodinamica Alpina, Padova) and RFBR (projects 00-15-98576 and 01-05-97234).

REFERENCES CITED

- Clark, J.R., Appleman, D.E., and Papike, J.J. (1969) Crystal-chemical characterization of clinopyroxenes based on eight new structure refinements. Mineralogical Society of America, Special Paper, 2, 31–50.
- Dal Negro, A., Carbonin, S., Molin, G., Cundari, A., and Piccirillo, E.M. (1982) Intracrystalline cation distribution in natural clinopyroxenes of tholeiitic, transitional and alkaline basaltic rocks. In S.K. Saxena, Ed., *Advances in Physical Geochemistry*, 2, p. 117–150. Springer-Verlag, New York.
- Ibers, J.A. and Hamilton, W.C., Ed. (1974) *International Tables for X-Ray Crystallography*, Vol. IV. Kynoch, Birmingham, U.K.
- North, A.C.T., Phillips, D.C., and Mathews, F.S. (1968) A semi-empirical method of absorption correction. *Acta Crystallographica*, A24, 351–359.
- Ohashi, H. and Fujita, T. (1979) Crystal chemistry of kosmochlor-diopside solid solutions. *Journal Japanese Association of Mineralogy, Petrology, Economic Geology*, 74, 16–26.
- Ohashi, H. (1981) Studies of the Si-O distances in $NaM^{3+}Si_2O_6$ pyroxenes. *Journal Japanese Association of Mineralogy, Petrology, Economic Geology*, 76, 308–311.
- Ohashi, H., Osawa, T., and Sato, A. (1994) $NaVSi_2O_6$. *Acta Crystallographica*, C50, 1652–1655.
- Reznitskii, L.Z. and Sklyarov, E.V. (1996) Unique Cr-V mineral association in metacarbonate rocks of the Sludyanka, Russia. 30th International Geological Congress, Beijing, China. Abstract, 2–3, 446.
- Reznitskii, L.Z., Sklyarov, E.V., and Ushchapovskaya, Z.F. (1985) Natalyite $Na(V,Cr)Si_2O_6$, a new chromian-vanadian pyroxene from Sludyanka. *Proceedings Russian Mineralogical Society*, 114, 5, 630–635.
- Reznitskii, L.Z., Sklyarov, E.V., and Karmanov, N.S. (1998) Escolaite in metacarbonate rocks of the Sludyanka group, southern Baikal region. *Doklady Earth Sciences*, 363, 8, 1049–1053.
- (1999) The first find of kosmochlor (ureyite) in metasedimentary rocks. *Doklady Earth Sciences*, 364, 1, 64–67.
- Shannon, R.D. (1976) Revised effective ionic radii and systematic studies of interatomic distances in halides and chalcogenides. *Acta Crystallographica*, A32, 751–767.
- Sheldrick, G.M. (1993) Shelxl-93. Program for crystal structure refinement. Gottingen University, Germany.
- Tokonami, M. (1965) Atomic scattering factor for O^{2-} . *Acta Crystallographica*, 19, 486.

MANUSCRIPT RECEIVED APRIL 4, 2001

MANUSCRIPT ACCEPTED DECEMBER 24, 2001

MANUSCRIPT HANDLED BY ROBERTA OBERTI